Journal of Mines, Metals and Fuels, *73(10): 3215-3225; 2025. DOI: 10.18311/jmmf/2025/49754*

Online ISSN : 0022-2755

Journal of Mines, Metals and Fuels

Contents available at: *www.informaticsjournals.co.in/index.php/jmmf*

Thermomechanical Buckling Response of Homogeneous and Functionally Graded Aluminium Beams Using Reddy's Higher-Order Theory

C. Naga Kumar[1], N. Leela Prasad[2], K. Chandra Shekar[2], N. Keerthi[3*] and Ch. Ravikiran[4]

[1]Department of Mechanical Engineering, G. Pullaiah College of Engineering and Technology, Kurnool - 518452, Andhra Pradesh, India

[2]Department of Mechanical Engineering, Vignan Institute of Technology and Science, Deshmukhi, Hyderabad - 508284, Telangana, India

[3]Department of Mechanical Engineering, Annamacharya University, Rajampet - 516126, Andhra Pradesh, India; aits.med.nk@gmail.com

[4]Department of Mechanical Engineering, MLR Institute of Technology, Hyderabad - 500043, Telangana, India

Abstract

This study aims to investigate the thermal buckling behaviour of thick homogeneous and functionally graded aluminium-based beams using Reddy's higher-order shear deformation theory. Recognising the limitations of classical and first-order theories in capturing shear effects and temperature-induced material degradation, a refined numerical model was developed to assess the stability of aluminium beams reinforced with Al_2O_3 and TiC under thermal loading. The material properties were assumed to vary through the beam thickness according to a power-law distribution, and temperature-dependent stiffness degradation is incorporated to mimic realistic high-temperature conditions. Three beam configurations, viz. a homogeneous aluminium beam, an Al-Al_2O_3 FG beam, and an Al-TiC functionally graded beam, were analysed over a temperature range of 30°C to 430°C and multiple gradation indices. The core novelty lies in the unified application of Reddy's higher-order shear deformation theory combined with temperature-sensitive gradation to evaluate and compare the thermal buckling response across these three configurations. The results revealed a clear decline in critical buckling load with rising temperature across all cases. Functionally graded beams demonstrated superior buckling resistance compared to the homogeneous counterpart, with the Al-TiC configuration showing the highest critical buckling load values due to the high stiffness and thermal resilience of TiC. Among all gradation profiles, a lower power-law index (k = 1) emerged as optimal, offering up to 246% enhancement in critical buckling load. This work underscored the advantages of material gradation in enhancing thermal stability and validated the effectiveness of Reddy's higher-order shear deformation theory in modelling thermomechanical instability in advanced composite beams. The insights gained can enhance the design of high-temperature structural components for aerospace, energy, and defence applications.

Major Findings: *The study proved that functionally graded beams reinforced with TiC demonstrated 246% more thermal buckling resistance than homogeneous aluminium beams. Optimal performance was observed at lower gradation indices (k = 1), where ceramic content near the compressive region enhanced stiffness. Reddy's higher-order shear deformation theory proved effective in accurately capturing nonlinear shear effects and temperature-dependent material degradation.*

Keywords: *Alumina, Aluminum, Functionally Graded Beam, Reddy's HSDT, Thermal Buckling, Titanium Carbidey*

**Author for correspondence*

1.0 Introduction

Buckling is a critical failure mode in structural components in slender and moderately thick elements subjected to compressive forces. The classical Euler theory works for slender beams, but it is inapplicable when, due to the inability to ignore shearing deformations. It fails when applied to thicker sections[1]. In this respect, First-order Shear Deformation Theories (FSDT) are also not satisfactory as they are based on empirical shear correction factors to relate shear strains to shear deformations[2]. More complex models have become a focus of more attention as they can achieve higher accuracy in predicting the mechanical behaviour of thick beams, when thermal and/or mechanical loading induces nonlinear bending and shear responses[3-5].

Thermal conditions that include high temperatures or non-uniform temperature distributions are also crucial due to their implications on the stability of the physical components. Another concern is that the materials become less stiff with temperature, and differential expansion can create large thermal stresses that may lead to premature buckling[6]. This is a problem with thick structures, as major temperature differences occur through the thickness of the structure. Functionally Graded Materials (FGM) are a new class of materials developed to meet this requirement, providing the ability to achieve property changes that are gradual from a ductile metal on one surface and a stiff ceramic on the other surface[7-9]. This gradation not only enhances thermal resistance but also reduces stress concentrations, which makes FGM ideal for high-temperature applications[10].

The Euler-Bernoulli and Timoshenko analytical methods have served as established tools for buckling analysis. Euler's model is effective for slender beams as it neglects shear deformation entirely, making it unsuitable for thick beams where such effects are significant[11]. FSDT enhances this by including shear deformation, but it requires the use of empirical shear correction factors to account for non-uniform shear strain through the thickness[12]. Whenever the temperature or position affects material properties, thermomechanical problems encounter limitations due to the necessity of correction factors.

Higher-Order Shear Deformation Theories (HSDT) have gained prominence in recent times. Third-order shear deformation theory by Reddy stands out for its ability to model realistic parabolic shear strain distributions without needing correction factors[13]. This theory inherently satisfies the shear stress-free boundary conditions at the top and bottom surfaces of the beam. Reddy's model has been extensively adopted in the literature for analysing thick, laminated, and thermally loaded beams and plates[14,15]. This method functions effectively for studying buckling behaviour of complex geometrical objects and non-homogeneous materials through its ability to work with temperature-sensitive structures[16].

Researchers have studied beam and plate buckling under thermal and mechanical loads through different analytical and numerical models. The thermal buckling analysis of isotropic, laminated and functionally graded structures has been widely adopted using Reddy's theory. This methodology has been recently extended to FGM, where properties vary smoothly through the thickness. Kenanda *et al.*[17] proposed a modified exponential shear deformation theory to study the free vibration, buckling, and bending behaviour of exponential functionally graded beams under various boundary conditions. Pu *et al.*[18] used HSDT to investigate the natural frequencies of sigmoid functionally graded sandwich beams. Belkhodja *et al.*[19] conducted a study on the buckling behaviour of Functionally Graded (FG) sandwich beams with porous ceramic cores through their framework built with third-order shear deformation theory. Research has been conducted by Pham *et al.*[20] to study free vibration responses of multi-directional structures through HSDT analysis while investigating various grading patterns and directions. Belarbi *et al.*[21] developed a hyperbolic form of HSDT to analyse both buckling and free vibration responses of isotropic and functionally graded sandwich beams under a range of boundary conditions. Khare *et al.*[22] used a finite element model grounded on an advanced parabolic shear deformation theory to examine the vibrational and buckling characteristics of functionally graded sandwich beams. Quasi-3D theories were developed as an extension of HSDT to more accurately describe the behaviour of functionally graded sandwich beams, especially by including the influence of transverse normal stress. These models are more accurate and reliable because each incorporates thickness-stretching effects in the transverse displacement via higher-order shear shape functions. Kanıg *et al*[23], analytical solutions for the bending and buckling analysis of functionally

graded beams using HSDT. Mohamed *et al.*[24] employed a novel higher-order shear and normal deformation theory for the analysis of free vibration and buckling of functionally graded sandwich beams under various boundary conditions.

While numerous studies have applied Reddy's HSDT to analyse the buckling and vibration behaviour of functionally graded beams, most prior work has focused predominantly on conventional ceramic reinforcements such as SiC and Al_2O_3 under simplified thermal or mechanical loading. In contrast, the present study introduces TiC as a high-performance ceramic phase, which has received limited attention in FGM buckling analyses despite its superior stiffness and thermal resistance.

Furthermore, this work incorporates temperature-dependent material degradation into the mechanical modelling, enabling a more realistic prediction of thermal buckling behaviour. Unlike previous models that assume temperature-invariant stiffness, our framework captures progressive stiffness reduction across a wide thermal range (30°C - 430°C). The study also provides a direct comparative evaluation between Al-Al_2O_3 and Al-Al-TiC Functionally Graded Beams (FGB), as well as a baseline homogeneous aluminium beam, offering new insights into how reinforcement type and gradation index influence buckling resistance under thermal loads. This combination of TiC-based functional gradation, temperature-sensitive stiffness modelling, and three-system comparative analysis using HSDT represents a novel and comprehensive contribution to the field of thermomechanical stability of graded structures.

The present study aims to investigate and compare the thermal buckling behaviour of homogeneous and functionally graded thick beams using Reddy's HSDT. A numerical formulation is developed based on Reddy's third-order theory that captures the nonlinear variation of transverse shear strain without the need for empirical correction factors. The study incorporates temperature-dependent degradation of material stiffness by modelling Young's modulus as a function of temperature, which enables a realistic representation of thermomechanical behaviour. The analysis focuses on two beam configurations: a homogeneous aluminium beam and a functionally graded Al-Al_2O_3 beam subjected to identical boundary and thermal loading conditions.

2.0 Materials and Methodology

2.1 Materials

The present study investigates three different beam configurations, which include a Homogeneous Aluminium Beam (HB) together with two FGB types made from aluminium and ceramic reinforcements: lumina (Al_2O_3) (FGB1) and Titanium Carbide (TiC) (FGB2). The chosen materials are commonly used in aerospace and high-temperature structural components because they demonstrate essential resistance to thermal and mechanical stresses.

The homogeneous beam uses Aluminium as its base material because it provides lightweight properties, excellent thermal conductivity, and good mechanical strength. The material exhibits a substantial reduction in stiffness when exposed to elevated temperatures, which requires evaluation against graded composites[25]. Al_2O_3 demonstrates high stiffness together with superior thermal resistance while displaying brittle characteristics. The graded inclusion of Al_2O_3 within aluminium produces strengthened thermal load-bearing capacity while it reduces stress concentrations across the depth of the beam[26]. TiC provides better hardness and high thermal stability, and its application in functional gradation is expected to increase resistance against thermal buckling and improve stiffness. The TiC addition introduces a material system with a higher thermo-mechanical property that enables a wider exploration of gradation effects[27]. Power-law distribution forms the basis of the FGB construction because it changes the material volume fractions from metal to ceramic across the thickness of the beam. By tailoring these materials across the thickness, the structure improves both performance and thermal stress distribution to prevent emergency buckling in the presence of temperature gradients. The properties of Aluminium, Al_2O_3 and TiC are provided in Table 1.

Table 1. Properties of the materials under consideration

Property	Aluminium	Al_2O_3	TiC
Young's Modulus (GPa)	70	225	400
Poisson's Ratio	0.32	0.27	0.23
Coefficient of thermal expansion ($^oC^{-1}$)	20×10^{-6}	8×10^{-6}	9×10^{-6}

2.2 Reddy Beam Theory for Homogeneous Beam with Thermo-Mechanical Loads

The mechanical stability of homogeneous beams under axial compressive loads is fundamentally governed by their resistance to buckling, which depends on both material stiffness and geometrical configuration. For slender beams, Euler-Bernoulli theory suffices; however, for moderate-to-thick beams, the HSDT provides improved fidelity by incorporating transverse shear effects without the need for shear correction factors. The beam considered in this study is a moderately thick, prismatic structure made entirely of aluminium and subjected to axial compressive loading under a uniform thermal gradient. The beam is modelled with a dimensionless length (L) of 1, a height (h) of 0.3, and a width (b) of 0.3. To capture realistic deformation behaviour, it is assumed that the beam is isotropic and homogeneous in material distribution. Unlike classical Euler-Bernoulli assumptions, which neglect shear deformation, the present analysis employs Reddy's HSDT, allowing for a cubic variation of transverse shear strain through the thickness. This approach inherently satisfies the shear stress–free boundary conditions at the top and bottom surfaces without invoking empirical correction factors. The neutral axis of the beam is assumed to remain straight, but cross-sections may warp and do not remain perpendicular to the deformed axis-capturing the essential features of thick beam behaviour under thermomechanical loading.

2.2.1 Governing Assumptions

The following assumptions are made during the analysis of HB:

- The beam is made of isotropic and homogeneous material.
- Plane sections do not remain perpendicular to the neutral axis after deformation (as in a classical theory) but include a higher-order shear strain variation.
- The top and bottom surfaces of the beam are shear stress-free, naturally satisfied by the higher-order function used in HSDT.

The schematic representation of the HB of Aluminium undertaken in the present research work is presented in Figure 1. The position boundary conditions applied in the current research are simply supported conditions at both ends of the beam.

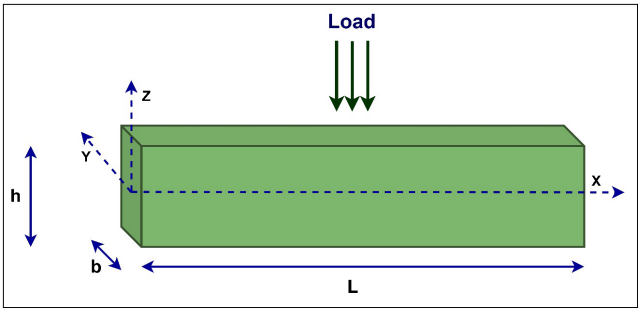


Figure 1. Homogeneous beam of aluminium.

2.2.2 Axial and Thermal Buckling Load

The shear strain distribution ($\gamma_{xz}(z)$) using Reddy's HSDT is estimated using Equation (1), which satisfies the zero shear stress conditions $z = \pm h/2$.

$$\gamma_{xz}(z) = \left(1 - \frac{4z^2}{h^2}\right)\frac{dw}{dx} \tag{1}$$

The effective bending rigidity (D) is estimated using Equation (2).

$$D = b\int_{-h/2}^{+h/2} E(z) \times z^2 dz \tag{2}$$

The effective shear rigidity (K_s) is estimated using Equation (3).

$$K_s = b\int_{-h/2}^{+h/2} \frac{E(z,T)}{2(1+\vartheta(z))}\left(1 - \frac{4z^2}{h^2}\right)^2 dz \tag{3}$$

The critical buckling load (P_{cr}) can be estimated using Equation (4).

$$P_{cr} = \frac{\pi^2 D}{(KL)^2} + K_s \tag{4}$$

Under varying temperature conditions, the material properties of the beam can be estimated using Eqsuations (5) to (7).

$$E(T) = E_0\,[1 - \beta_E \times (T - T_{ref})] \tag{5}$$

$$\rho(T) = \rho_0\,[1 - \beta_E \times (T - T_{ref})] \tag{6}$$

$$\vartheta(T) = \vartheta_0\,[1 - \beta_E \times (T - T_{ref})] \tag{7}$$

Here, $E(T)$, $\rho(T)$, and $\vartheta(T)$ are the Young's modulus, density and Poisson's ratio of the beam material. E_0, ρ_0, and ϑ_0 are their respective values at the reference temperature T_{ref}. β_E is the temperature sensitivity coefficient.

2.3 Reddy Beam Theory for Functionally Graded Beam with Thermo-Mechanical Loads

2.3.1 Reddy's Theory for Beam

The material gradation in functionally graded beams is modelled using a power-law distribution of volume fractions through the beam thickness. This approach assumes that the volume fraction of the ceramic phase varies continuously from the top to the bottom surface according to the power-law index K, as shown in Equations (8)-(10). This assumption is well-established in FGM literature and offers flexibility in tailoring material transitions between metal and ceramic constituents[5]. Compared to other gradation laws (e.g., exponential or sigmoid), the power-law provides a balance between physical realism and analytical tractability, making it especially suitable for closed-form solutions and finite element formulations[11]. Moreover, power-law models have been experimentally validated in numerous fabrication techniques, such as powder metallurgy and spark plasma sintering, which yield continuous microstructural transitions consistent with such profiles. Therefore, the use of power-law distribution is both mathematically robust and practically representative of FGM behaviour in aerospace and structural applications[13]. The present study uses Reddy's HSDT to model a beam that transitions from aluminium (Al) to alumina (Al_2O_3). The beam material properties change from one end to the other through a power-law distribution as shown in Equations (8) to (10)[28].

$$E(z) = E_m + (E_c - E_m)\left(\frac{z+\frac{h}{2}}{h}\right)^k \tag{8}$$

$$\rho(z) = \rho_m + (\rho_c - \rho_m)\left(\frac{z+\frac{h}{2}}{h}\right)^k \tag{9}$$

$$\vartheta(z) = \vartheta_m + (\vartheta_c - \vartheta_m)\left(\frac{z+\frac{h}{2}}{h}\right)^k \tag{10}$$

Here, E, V, ρ, and ϑ represents the Young's modulus, volume fraction, density, and Poisson's ratio. m and c refer to the metallic (Al) and ceramic (Al_2O_3) phases, respectively, and k is the power-law index controlling the gradation profile.

The HSDT of Reddy is used because it can handle transverse shear deformation without the need for empirical shear correction factors. The theory assumes a cubic variation of transverse shear strain through the beam thickness, which inherently satisfies the zero shear stress conditions at the upper and lower surfaces as given in Equation (11)[29].

$$\frac{d\varnothing(z)}{dz} = 1 - \frac{4z^2}{h^2} \tag{11}$$

Effective bending (EI_{eff}) and shear (k_{seff}) stiffnesses are numerically evaluated through thickness integration of these variable material properties, accounting for temperature-dependent property degradation. This rigorous approach allows accurate prediction of the critical thermal buckling load and effectively highlights the influence of material gradation under various thermal scenarios. The model of FGB is presented in Figure 2. Again, the position boundary conditions applied are considered to be simply supported conditions at both ends of the beam.

Classical beam theory often neglects transverse shear deformation entirely, making it unsuitable for moderately thick or deep beams. While the First-order shear deformation theory partially addresses this by incorporating shear deformation, it relies on empirical shear correction factors, which are often inaccurate for non-homogeneous and thermally loaded materials. In contrast, Reddy's HSDT captures a realistic parabolic distribution of shear strains through the beam thickness and inherently satisfies the shear stress-free boundary conditions without correction factors. This makes HSDT particularly effective for analysing functionally graded beams and structures under thermal gradients, where both material and geometric nonlinearities significantly influence buckling performance. Given the complexity of

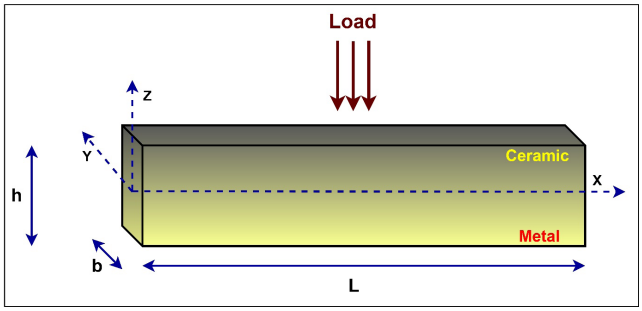


Figure 2. The model of FGB.

functionally graded materials and temperature-dependent stiffness degradation, HSDT offers the most physically accurate and computationally reliable methodology for this study.

2.3.2 Temperature Field and Material Degradation

A linear temperature distribution $T(z)$ is assumed through the beam thickness from T_{bot} at the bottom surface to T_{top} at the top[30]. The degradation of Young's modulus due to temperature is modelled by a linear relationship as shown in Equation (12).

$$E(z,T) = E(z)[1 - \beta_E \times (T(z) - T_{ref})] \quad (12)$$

β_E is the temperature sensitivity coefficient and T_{ref} is the reference temperature at which the mechanical properties of the beam are known.

This simplified linear relationship has been widely adopted in thermal buckling studies due to its balance between accuracy and computational efficiency[30]. It effectively reflects the progressive stiffness degradation of aluminium and ceramic materials in the 30 - 430°C range, which aligns with their operational thresholds in aerospace and automotive applications. The temperature range and degradation model used in this study are therefore deemed realistic and suitable for evaluating thermomechanical performance in high-temperature scenarios.

The effective bending rigidity and shear rigidity are calculated using Equations (13) and (14).

$$EI_{eff} = b\int_{-h/2}^{+h/2} E(z,T)\times z^2 dz \quad (13)$$

$$K_s = b\int_{-h/2}^{+h/2} \frac{E(z,T)}{2(1+\vartheta(z))}\left(\frac{d\varnothing}{dz}\right)^2 dz \quad (14)$$

2.3.3 Thermal Axial Force and Buckling Load

The thermal axial force induced by temperature gradients is evaluated using Equation (15).

$$N_T = b\int_{-h/2}^{+h/2} E(z,T)\times\alpha(z)\times(T(z)-T_{ref})dz \quad (15)$$

The P_{cr} under thermo-mechanical loading is computed using Equation (16).

$$P_{cr} = \frac{\pi^2 EI_{eff}}{(KL)^2} - N_T + K_s \quad (16)$$

2.4 Justification for the Chosen Temperature Range

The selected temperature range of 30°C to 430°C is motivated by practical service conditions encountered in aerospace, automotive, and high-temperature industrial components, where metallic and composite structural members are frequently subjected to ambient-to-elevated thermal environments[31]. The lower bound (30°C) corresponds to standard laboratory conditions, while the upper limit (430°C) approaches the operational thermal thresholds for aluminium-based alloys, beyond which significant stiffness degradation and phase instability may occur. This range captures the onset and progression of thermal softening, allowing for a realistic assessment of buckling behaviour across mild to severe thermal loads. Additionally, it facilitates comparison between homogeneous and functionally graded configurations under temperature-dependent mechanical deterioration, thereby providing critical insight into the thermal resilience of graded material systems.

The imposed axial compressive load mirrors the prevalent buckling failure mode observed in components like fuselage frames, heat shields, and support beams operating under combined thermal and mechanical stresses. These components must be dimensionally stable and must be able to support critical loads while experiencing thermal changes and having constrained ends, where buckling becomes the primary failure mode. In this context, the load and temperature considerations are chosen to provide a practical and applicable approach in assessing the structural performance of functionally graded aluminium-based composites.

2.5 Comparative Analysis of the Mechanical Performance

To quantify the effect of material gradation and reinforcement on the thermo-mechanical stability of beams, a comparative analysis was carried out with three configurations: a homogeneous aluminium beam and two functionally graded beams reinforced with Al_2O_3 and TiC, respectively. Each model was analysed under identical geometric dimensions, boundary conditions, and thermal environments. The comparison of P_{cr} was based on variations in the gradation index and temperature-dependent degradation of material properties. This systematic evaluation enabled a deeper understanding of how gradation profile and ceramic reinforcement collectively affect the mechanical behaviour of thick beams subjected to thermal and compressive loads.

3.0 Results and Discussion

The thermal buckling performance, P_{cr}, in the temperature range of 30°C to 430°C for the HB is presented in Table 2. P_{cr} steadily declines with temperature rise, reducing from 1.74 MN at ambient conditions to 1.46 MN at the highest temperature under consideration. This nearly 16.0% reduction encapsulates the thermal vulnerability of aluminium, a material known for its appreciable strength-to-weight ratio but diminished stiffness retention at elevated temperatures[32]. The decrease in P_{cr} can be attributed to the significant deterioration of Young's modulus with temperature[33]. In the absence of any reinforcing phase or gradient structure to redistribute thermal stresses, the aluminium beam uniformly undergoes stiffness degradation, thereby compromising its buckling resistance. Furthermore, as a monolithic structure, it lacks the mechanical buffering mechanisms typically introduced by functionally graded architectures, such as stress delocalisation or stiffness enhancement near critical regions[34].

The HB presents considerable limitations under thermo-mechanical loading conditions, but serves as a baseline model to quantify and prove the superiority of FG beams reinforced with alumina or titanium carbide.

Table 2. Results of the homogeneous beam

Temperature	30	130	230	330	430
P_{cr} (kN)	1739066	1669503	1599941	1530378	1460816

Table 3. Results of the FGB-1

Power Law Index	P_{cr} at different temperatures (kN)				
	30	130	230	330	430
1	3720340	3555024	3391084	3228518	3067328
2	2984258	2849497	2716019	2583823	2452910
3	2619030	2499587	2381367	2264371	2148599
4	2408695	2298131	2188753	2080558	1973549
5	2275386	2170481	2066733	1964143	1862711

These findings strongly support the incorporation of material gradation strategies in structural systems intended for thermally demanding environments.

Table 3 presents the thermal buckling behaviour of the FGB-1 at different values of gradation indices (k = 1 to 5), in the temperature range of 30°C to 430°C. The results showcase a consistent decline in P_{cr} with temperature elevation, an outcome primarily driven by temperature-induced degradation in material stiffness. Irrespective of the gradation index, the highest P_{cr} is observed at ambient temperature (30°C), while the lowest values occur at the highest temperature (430°C), thus demonstrating the pronounced thermal sensitivity of the system. Notably, a lower power-law index (k = 1) signifies a higher ceramic content near the top surface, thereby yielding superior buckling resistance due to enhanced stiffness contribution from alumina. The P_{cr} reaches a peak of 3.72 MN at 30°C for k = 1, significantly outperforming the homogeneous aluminium beam by more than 110%. As the gradation index increases, the influence of the ductile aluminium matrix becomes dominant, gradually diminishing the structural stiffness and thus the buckling capacity[35]. By k = 5, where ceramic content is minimal near the compressive side, the P_{cr} drops to 2.27 MN at 30°C, reflecting a 38.8% reduction compared to k = 1. This result underscores the role of tailored gradation in improving structural performance under thermomechanical loading. The gradual transition from metal to ceramic creates a beneficial stiffness gradient, which delays instability[36]. However, the benefit diminishes with increasing metallic dominance in the gradation profile. Therefore, k = 1 emerges as the optimal gradation for maximising thermal buckling resistance in the Al-Al_2O_3 system under the present conditions.

Table 4 details the P_{cr} values for the FGB-2, evaluated across temperatures from 30°C to 430°C and gradation

Table 4. Results of the FGB-2.

Power Law Index	P_{cr} at different temperatures (kN)				
	30	130	230	330	430
1	6005549	5738500	5473687	5211109	4950766
2	4408718	4209756	4012678	3817484	3624175
3	3621408	3456344	3292963	3131267	2971254
4	3169567	3024099	2880188	2737834	2597037
5	2883805	2750813	2619291	2489239	2360656

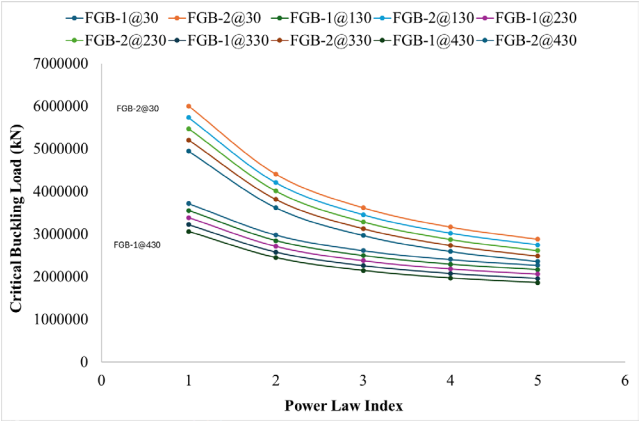


Figure 3. P_{cr} vs. Power law index at different combinations.

indices ranging from 1 to 5. The trend presented in Figure 3 showcases that, P_{cr} consistently declines with a rise in temperature due to the temperature-sensitive degradation of elastic modulus. However, the overall buckling resistance of Al-TiC beams is markedly higher compared to Al-Al_2O_3, highlighting the superior stiffness and thermal stability imparted by titanium carbide reinforcement[37]. At a gradation index of k = 1, which indicates a ceramic-rich upper region, the beam exhibits the highest P_{cr} of approximately 6.01 MN at 30 °C. This value represents an impressive gain of nearly 246% over the homogeneous aluminium beam, revealing the robustness of the TiC reinforcement in counteracting thermal softening. As the gradation index increases to k = 5, a progressive decline in P_{cr} is observed, culminating in a minimum of 2.36 MN at 430 °C. This transition reflects the increased dominance of aluminium in the load-bearing region, which compromises the beam's resistance to instability under axial compression[38]. Comparatively, the Al–TiC beam outperforms the Al-Al_2O_3 configuration across all temperatures and gradation indices, reaffirming TiC's advantage in high-temperature structural applications. The dense microstructure and high thermal modulus of TiC contribute to improved load transfer and resistance to thermal-induced distortion[37]. Therefore, FGB2 not only demonstrates superior thermal buckling strength but also offers design flexibility by tuning the gradation index for tailored mechanical performance.

To synthesise the thermal buckling performance across all beam types, a direct comparison at 30°C reveals the following: the P_{cr} for the homogeneous aluminium beam is 1.74 MN, whereas FGB1 with k = 1 reaches 3.72 MN, a 113.8% improvement. FGB2 with k = 1 further increases the P_{cr} to 6.01 MN, reflecting a 245.6% enhancement relative to the homogeneous case. These values confirm the profound effect of ceramic reinforcement and material gradation in delaying buckling failure. Across all gradation indices and temperature levels, FGB2 consistently outperforms both FGB1 and the HB, establishing TiC as the most effective reinforcement for thermal buckling resilience.

These findings emphasise the pivotal role of the gradation index k in governing the thermomechanical performance of FG beams. Physically, a lower k value concentrates a higher volume fraction of ceramic (Al_2O_3 or TiC) near the compressive top surface, enhancing stiffness where it is most needed to resist buckling. As k increases, the structure becomes more metal-rich near this region, which, while improving ductility and possibly manufacturability, compromises buckling resistance due to aluminium's lower stiffness and thermal resilience. From a design standpoint, this implies that tailoring the gradation index offers a controllable parameter to tune structural response under thermal and mechanical loading. For applications requiring maximum buckling resistance (e.g., aerospace heat shields, turbine blades), a low k value (e.g., k = 1) is optimal. Conversely, in scenarios where ductility, cost, or manufacturability dominate the design criteria, a moderate k may offer a better balance. These insights support the use of functionally graded architectures not just for structural integrity, but also for achieving application-specific performance targets.

The superior thermal buckling resistance observed in TiC- and Al_2O_3-reinforced functionally graded beams, particularly with low gradation indices, directly aligns with the structural performance requirements of aerospace, energy, and defence sectors. In aerospace, components such as fuselage panels, leading edges, and engine

supports are subjected to thermal gradients and axial compression, where delayed buckling is critical to flight integrity. Similarly, energy systems (e.g., thermal reactors, turbine casings, solar receivers) demand materials that maintain dimensional stability under high thermal loads. In defence applications, missile casings, armoured panels, and thermal shields benefit from structures that balance weight with thermal and mechanical robustness.

4.0 Effect of Boundary Conditions - Practical Implications

Although this study considers Simply Supported (SS) boundary conditions to facilitate comparison and analytical clarity, real-world components often experience different constraints, such as Clamped–Clamped (CC) or Clamped–Free (CF) ends. It is well established that clamped conditions increase structural stiffness, which generally leads to higher critical buckling loads compared to simply supported beams. For instance, under identical loading and material configurations, a CC beam could exhibit 30–60 % higher buckling resistance, depending on geometry and gradation profile[5,9,11].

5.0 Conclusions

This study presented a comprehensive thermomechanical buckling analysis of homogeneous and functionally graded aluminium-based beams employing Reddy's higher-order shear deformation theory. The inclusion of temperature-dependent material degradation and power-law gradation provided a realistic and detailed understanding of how structural behaviour evolves under thermal loading. Based on the comparative numerical results, the following key conclusions can be drawn:

- **Thermal sensitivity of homogeneous beams**: The critical buckling load of the homogeneous aluminium beam exhibited a consistent decline with increasing temperature, highlighting the intrinsic limitations of monolithic metals in high-temperature environments due to rapid stiffness degradation.
- **Performance gain through material gradation**: Functionally graded beams, particularly those reinforced with Al_2O_3 and TiC, demonstrated significantly enhanced buckling resistance. For instance, the Al–TiC beam at a low gradation index ($k = 1$) exhibited a critical buckling load enhancement of over 245% compared to the homogeneous beam at room temperature.
- **Influence of gradation index**: As the power-law index increased, the material distribution favoured aluminium near the compressive side, which reduced buckling capacity. The optimal configuration for both FG systems occurred at $k = 1$, indicating the critical role of ceramic reinforcement near the load-dominant regions.
- **TiC vs. Al_2O_3 reinforcement**: Among the two FG configurations, TiC-reinforced beams consistently outperformed those reinforced with Al_2O_3, owing to TiC's superior thermal modulus and mechanical strength, making it more suitable for applications exposed to high thermal gradients.
- **Suitability of Reddy's HSDT**: Reddy's third-order shear deformation theory proved to be efficient in capturing the realistic shear behaviour and transverse stiffness variations in the case of homogeneous as well as functionally graded beams with no reliance on empirical correction factors.

This investigation proves that employing ceramic reinforcement with tailored gradation can enhance the structural stability of beams under thermo-mechanical loads. By optimising gradation profiles, designers can mitigate buckling risks in high-temperature environments while balancing weight, manufacturability, and mechanical performance.

6.0 References

1. Gupta P, Singh B, Shrivastava Y, Kumar S. Multiquadric collocations for nonlinear vibration of functionally graded plates of Ti-6Al-4V metal. J Mines Met Fuels. 2023; 71(12B):252-260. https://doi.org/10.18311/jmmf/2023/45590
2. Van NT, Van Minh P, Duc ND. Finite-element modelling for static bending and free vibration analyses of double-layer non-uniform thickness FG plates taking into account sliding interactions. Arch Civ Mech Eng. 2024; 24(2):107. https://doi.org/10.1007/s43452-024-00914-9
3. Reddy G, Valiveti S, Hussain S. Comparative Investigation of deflection in a two-directional functionally graded porous curved and straight beams adapting unified shear deformation theory. J Comput Appl Mech. 2025; 56(1):145-161.

4. Kannaiyan GN, Balasubramaniam V, Pappula B, Makgato S. Critical buckling analysis of functionally graded porous beam using Karush-Kuhn-Tucker conditions. Buckling Analysis. 2025; 10(1).
5. Chintalapudi R, Kannaiyan GN, Pappula B, Makgato S. The novel Vogel's approximation method integrated with a random forest algorithm in the vibration analysis of a two-directional functionally graded taper porous beam: Assessment. Sci Afr. 2024; 26:e02397. https://doi.org/10.1016/j.sciaf.2024.e02397
6. Mohana Reddy GC, Kiran R, Nagaraju S, Bridjesh P. On numerical analysis of refined higher-order shear deformation theory for frequency responses of two-directional functionally graded taper beams. Acad J Manuf Eng. 2024; 22(2):109-120.
7. Chintalapudi R, Kannaiyan GN, Pappula B, Makgato S. The effects of gradient index, aspect ratio, porosity, and boundary conditions on the buckling behaviour of functionally graded porous beams: A k-out-of-n system reliability analysis. Results in Physics. 2024; 60:107634. https://doi.org/10.1016/j.rinp.2024.107634
8. Geetha KN, Balasubramaniam V, Pappula B, Makgato S. Novel Kuhn-Tucker conditions for vibration analysis in a functionally graded porous beam using the R program. Results iEng. 2024; 22:102064. https://doi.org/10.1016/j.rineng.2024.102064
9. Bridjesh P, Geetha NK, Reddy G. On numerical investigation of buckling in two-directional porous functionally graded beam using higher order shear deformation theory. Mech Adv Compos Struct. 2023; 10(2):393-406.
10. Han G, Wan M, Su A, Li B. Thermal buckling and post-buckling behaviour of FGM laminate plates reinforced with graphene nanoplatelets. Multiscale Multidiscip Model Exp Des. 2025; 8(5):256. https://doi.org/10.1007/s41939-025-00810-6
11. Geetha NK, Bridjesh P, Yelamasetti B, Saxena KK, Gupta N. Analytical modelling of a multifunctional heterogeneous beam-bending analysis. Proc Inst Mech Eng, Part E. 2023; 0(0). https://doi.org/10.1177/09544089231207421
12. Jain R, Azam MS. Effect of partial elastic foundation on the bending behaviour of functionally graded tapered porous plates utilizing Rayleigh-Ritz approach and deformation prediction with artificial neural network. Int J Interact Des Manuf (IJIDeM). 2025. https://doi.org/10.1007/s12008-024-02178-2
13. Bridjesh P, Geetha NK, Yelamasetti B. Numerical investigation on buckling of two-directional porous functionally graded beam using higher order shear deformation theory. Int J Interact Des Manuf. 2024; 18:2805-2818. https://doi.org/10.1007/s12008-023-01332-6
14. Gajbhiye PD, Yelve N, Ghugal YM, Das AK. Displacement and stress analysis of laminated and sandwich beams under various mechanical loads using a quasi-2D theory. Arch Appl Mech. 2025; 95(2):47. https://doi.org/10.1007/s00419-024-02751-x
15. Wang Z, Meng Q. An Analytical study on the thermal post-buckling behaviours of geometrically imperfect FRC-laminated beams using a modified zig-zag beam model. Aerospace. 2025; 12(2):138. https://doi.org/10.3390/aerospace12020138
16. Bridjesh P, Chandra Mohana Reddy G, Geetha NK, Ravikiran Ch, Nagaraju S. On numerical buckling analysis of two-directional porous functionally graded beam using higher order shear deformation theory. Acad J Manuf Eng. 2023; 21(1):105-119.
17. Kenanda MA, Hammadi F, Zouari W, Belabed Z, Ayad R. Thermo-mechanical free vibration analysis of porous solar FGM plates resting on Kerr's foundation using a new logarithmic-hyperbolic shear deformation theory. Arch Appl Mech. 2025; 95(4):91. https://doi.org/10.1007/s00419-025-02779-7
18. Pu Y, Teng Z, Liu J, Li K, Luo Y. A generalized beam theory for bending analysis of functionally graded sandwich beams using a modified GDQ method. Mech Adv Mater Struct. 2025. https://doi.org/10.1080/15376494.2025.2467239
19. Belkhodja ME, Chorfi SM, Belalia SA, Belkhodja Y. Bending and free vibrations analysis of sandwich beams with porous functionally graded face sheets and a graphene platelets-reinforced aluminium core using a new quasi-3D beam theory. J Vib Eng Technol. 2025; 13(1):122. https://doi.org/10.1007/s42417-024-01646-z
20. Pham QH, Tran VK, Nguyen PC. Linear finite element formulation for free vibration and buckling analyses of multi-directional FGP doubly curved shallow shells in thermal environment. Sh Offshore Struct. 2025; 20(1):77-98. https://doi.org/10.1080/17445302.2024.2335440
21. Belarbi MO, Benounas S, Li L, Van Vinh P, Garg A. Vibration of a functionally graded doubly curved shallow nanoshell: An improved FSDT model and its nonlocal finite element implement. J Vib Eng Technol. 2025;13(1):93. https://doi.org/10.1007/s42417-024-01733-1
22. Khare S, Kumar R, Sharma HK, Prasad RB, Markad K, Singh S, Tiwari AK, Ven S. Static response of laminated plate using new parabolic higher order shear deformation theory: A finite element approach. Journal of Computational Appl Mech. 2025; 56(1):101-126.

23. Kanığ D. Flexural analysis of functionally graded sandwich plates with a novel mixed finite element formulation using quasi-3D higher order shear deformation theory. Mech Advd Mater Struct. 2025; 1-22. https://doi.org/10.1080/15376494.2025.2486738
24. Mohamed I, Şimşek S, Kahya V. Free vibration and buckling analysis of functionally graded sandwich beams resting on a two-parameter elastic foundation using a quasi-3D theory. Sigma J Eng Nat Sci. 2025; 43(1):47-61. https://doi.org/10.14744/sigma.2025.00005
25. Chinthalapudi R, Jatavallabhula JK, Kannaiyan GN, PB, Makgato SS. Random forest algorithm integrated with an initial basic feasible solution in buckling analysis of a two-dimensional functionally graded porous taper beam. Mater Res Express. 2025; 12(6). https://doi.org/10.1088/2053-1591/addf17
26. Prashanth N, Swamy LR, Kumar S. Tribological behaviour of jute/vinyl ester composites impregnated with alumina filler. J Mines Met Fuels. 2025; 73(2). https://doi.org/10.18311/jmmf/2025/45484
27. Jafar MS, Mallick B, Hameed AS, Chakraborty A. Experimental analysis of machining performances of CNC milling using AlTiN coated tungsten carbide tool (WC). J Mines Met Fuels. 2023; 70(12):665-674.
28. Reddy GCM, Bridjesh P, Reddy BS, Reddy KVK. Comparison of deflection in two-directional functionally graded tapered beam. Mech Adv Compos Struct. 2024;11: 191-202.
29. Geetha NK, Reddy GCM, Bridjesh P. Higher order shear deformation theory for functionally graded porous beam - numerical free vibrational analysis. J Eng Sci Technol Rev. 2023; 16(5):59-68. https://doi.org/10.25103/jestr.165.08
30. Sudindra S, Deepak SA. Study of design and analysis of S-glass fiber reinforced epoxy polymer metal laminate composites in the application of propeller shafts. J Mines Met Fuels. 2023; 71(12B):261-268. https://doi.org/10.18311/jmmf/2023/45591
31. Gayen D. Thermo-elastic buckling and free vibration behavior of functionally graded beams with various materials gradation laws. Int J Interact Des Manuf. 2025; 19(7):5397-5416. https://doi.org/10.1007/s12008-024-02141-1
32. Saini R, Saini R. Thermal buckling analysis of nonuniform FG nanobeams: analytical and numerical solutions. J Mech Mater Struct. 2024; 19(5):837-855. https://doi.org/10.2140/jomms.2024.19.837
33. Valencia Murillo CE, Gutierrez Rivera ME, Celaya Garcia LD. Thermal–structural linear static analysis of functionally graded beams using reddy beam theory. Math Comput Appl. 2023; 28(4):84. https://doi.org/10.3390/mca28040084
34. Gayen D, Tiwari R, Chakraborty D. Thermo-Elastic Static Behavior of Functionally Graded Shafts with Different Material Gradation Patterns. J Vib Eng Technol. 2024; 12(8):8963-8978. https://doi.org/10.1007/s42417-024-01581-z
35. Sahoo B, Mehar K, Sahoo B, Sharma N, Panda SK. Thermal post-buckling analysis of graded sandwich curved structures under variable thermal loadings. Eng Comput. 2023; 39(2):1267-1283. https://doi.org/10.1007/s00366-021-01514-4
36. Bensaid I, Saimi A, Civalek Ö. Effect of two-dimensional material distribution on dynamic and buckling responses of graded ceramic-metal higher order beams with stretch effect. Mech Adv Mater Struct. 2024; 31(8):1760-1776. https://doi.org/10.1080/15376494.2022.2142342
37. Zhang J, Wang L, Zhao K, Qi Q, Hao Y, Zhang Y, Sun L, Zhan X. Non-uniform deformation response of Ti6Al4V/TiC functionally graded material under different composition gradient designs by direct energy deposition. Addit Manuf. 2025: 104885. https://doi.org/10.1016/j.addma.2025.104885